Plasma Wakefield Acceleration Experiments in Overdense Regime Driven by Narrow Bunches

T. Kozawa, T. Ueda, T. Kobayashi, M. Uesaka, K. Miya

Nuclear Engineering Research Laboratory, Faculty of Engineering, The University of Tokyo,

2-22 Shirakata-Shirane, Tokai-mura, Naka-gun, Ibaraki 319-11, Japan

A. Ogata, H. Nakanishi, T. Kawakubo, M. Arinaga, K. Nakajima

National Laboratory for High Energy Physics, Tsukuba, Ibaraki 305, Japan

H. Shibata

Research Center for Nuclear Science and Technology, the University of Tokyo,

2-22 Shirakata-Shirane, Tokai-mura, Naka-gun, Ibaraki 319-11, Japan

N. Yugami, Y. Nishida

Department of Electrical and Electronic Engineering, Utsunomiya University,

Ishii-machi, Utsunomiya, Tochigi 321, Japan

D. Whittum

Stanford Linear Accelerator Center, Stanford University, Stanford, California, USA

Y. Yoshida

Institute of Scientific and Industrial Research, Osaka University, Mihogaoka, Ibaraki, Japan

Abstract

Experiments of plasma wakefield acceleration driven by narrow bunches were performed in overdense regime at the University of Tokyo. Changes of energy and beam size of test bunches caused by the driven bunches were observed. Acceleration gradient about 1 MeV/m was observed.

Introduction

Plasma wakefield acceleration is one of the methods which are proposed in order to obtain an acceleration gradient high enough for the next generation of linear colliders[1]. The concept has been first tested experimentally in 1988 at the Argonne National Laboratory[2]. More recently, gradient of 20 MeV/m has been produced by a train of bunches from the 500 MeV linac at KEK[3].

In this experiments, we have investigated dependence of acceleration characteristics on the plasma density in the overdense regime, in which plasma density is higher than the beam density. The drive beams were narrow; in other words, the product of plasma wavenumber and the beam size was less than unity. Changes in size and energy of test bunches caused by drive bunches were studied as a function of plasma density.

Experimental

The wakefield accelerator [4] consists of two linacs, achromatic lines, plasma chamber and energy analyzer, as shown in Fig. 1. Beams from one linac excite wakefields in a plasma, while beams from the other linac witness the wakefields. The time interval between the two beams is controllable with an accuracy of 1 ps. Plasma was produced in a chamber with .15m diameter and .36m length by pulse discharges between four lumps of LaB_6 cathodes and the chamber[5]. The cathodes were heated by a 10V-80A direct current source. The discharge pulse had a voltage of 80-120V, a current of 10-20A, a duration of 2 ms and a rate of 12.5 Hz equal to the linac beam repetition rate. The multi-dipole field of permanent magnets, 0.7 kG at the inner surface of the air-cooled chamber, was applied to confine the plasma. Argon gas was filled the chamber for the plasma production. The plasma density was controlled by the gas flow controller, the cathode temperature and the discharge voltage. The plasma density and electron temperature were measured by a Langmuir probe. The electron temperature was found to be 2-3eV. We adopted differential pumping in order to isolate the linacs from the test section.

The beam energy was measured by a 45° bending magnet at the end of the plasma chamber and beam sizes and positions were measured by using phosphor screens (Desmarquest AF995R). The energies of the drive beams and test beams were 24.1 MeV and 16.6 MeV, respectively, and the respective charges in each bunch were 300-400 pC and 70-80 pC at the exit of the energy analyzer. Vertical and horizontal beam sizes of the drive bunch were around 1.5 mm.

Experimental results and discussion

Beam images on the phosphor screen at the exit of the energy analyzer were observed as a function of time delay between drive and test bunches. Figure 2 shows time dependence of energy shift, which was derived from the position in horizontal direction, at the plasma density of $7.86 \times 10^{11} cm^{-3}$. Figure 3 shows change of beam sizes in horizontal and vertical directions at the plasma density of $7.86 \times 10^{11} cm^{-3}$.

The delay dependences obtained experimentally were fit to the equation

$$f(t) = e^{-t/\tau}[a_1 sin(\omega t + \phi_1) + a_2 sin(2\omega t + \phi_2)]. \quad (1)$$

The $sin2\omega t$ term is phenomenological and was included to im-

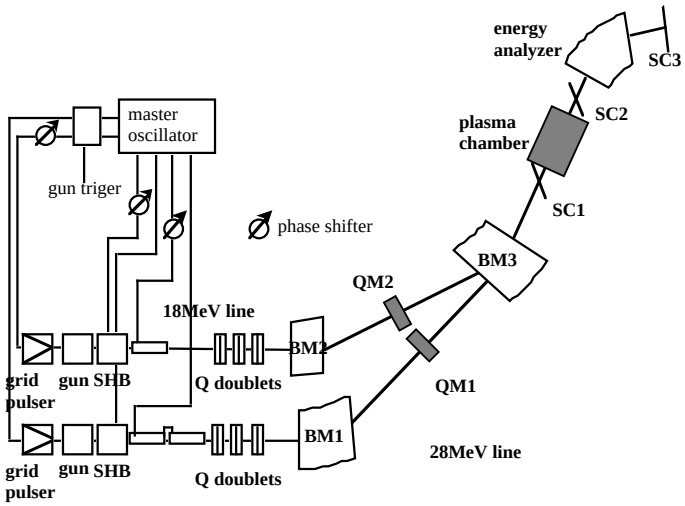

Figure. 1. Schematic diagram of the wakefield accelerator and positions of four phosphor screens SC1 to SC3.

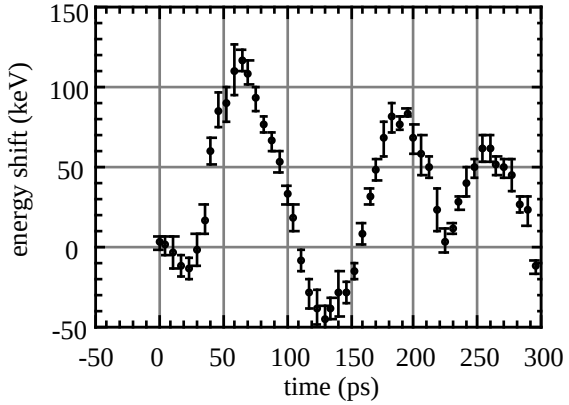

Figure. 2. Time dependence of energy change of test bunches at the plasma density of $7.86 \times 10^{11} cm^{-3}$.

prove the fit. Plasma frequencies and consequent plasma densities were derived from the ω values.

Measured plasma density distributions along the beam axis were shown in Fig. 4. The acceleration experiments were, however, performed in the density region far higher than those given in Fig. 4. The density distributions were then calculated by a similar method described in ref. [6]. This is possible because the damping characterized by τ in eq. 1 can be attributed to the heterogeneity of the density distribution as following. The plasma density and the resultant plasma frequency at the ends of the plasma column are lower than those at the plasma center. The test bunches suffer from the phase difference of the plasma oscillation, which becomes more severe as the time difference becomes longer. The phase difference tends to offset the positive and negative effects of the wakefield to decrease the amplitude of the oscillation.

In this specific data processing, a trapezoidal distribution was first assumed as n(z). The solid line in Fig. 4 shows the trapezoidal approximation of the distribution and data given by circle were obtained experimentally. The delay time dependence of the wakefield is then calculated by the relation

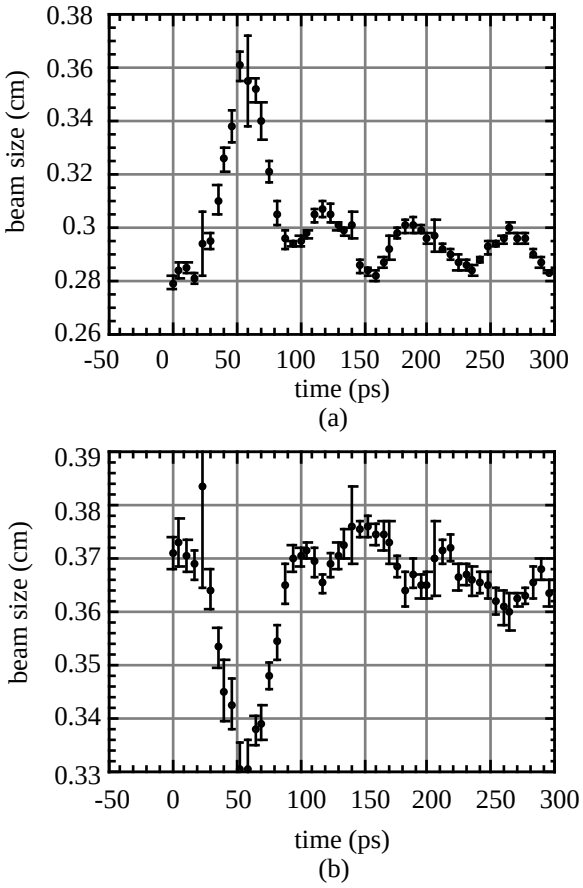

Figure. 3. Time dependence of beam sizes of test bunches in (a) horizontal and (b) vertical directions at the plasma density of $7.86 \times 10^{11} cm^{-3}$.

$$E(t) \sim \int_0^{L_0/2} -n(z) cos(\omega_p(z)t) dz, \quad (2)$$

where $\omega_p(z)$ is the plasma frequency, assumed to agree with ω in eq. 1 at the flat top of the trapezoidal distribution. The length of flat top of the trapezoid was adjusted so that its decay characteristics agree with the experimental data and the reduction of the wakefield amplitude was derived.

The acceleration gradient at the center of the distribution thus derived is given in Fig. 5. The solid line in the figure shows the prediction of linear theory,

$$W_z = -\frac{8 r_e mc^2 N}{a^2} exp[-\frac{k_p^2 \sigma_z^2}{2}][1 - \frac{4}{k_p^2 a^2} + 2K_2(k_p a)], \quad (3)$$

where N is the number of electrons in the drive bunch, k_p is the plasma wavenumber, σ_z is the bunch length, 1.2 mm, and a is the beam size, 1.5 mm.

The transverse wakefield caused by a drive bunch is given by

$W_r(r, \xi) = -\frac{16 r_e mc^2 N}{a^2}[K_2(k_p a) I_1(k_p r) - \frac{r}{k_p a^2}]$

$$\times exp(-\frac{k_p^2 \sigma_z^2}{2}) sin k_p \xi. \quad (4)$$

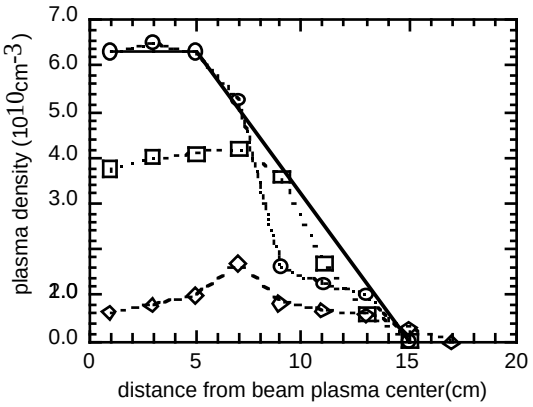

Figure. 4. Plasma density distributions along the beam axis. The solid line shows trapezoidal approximation.

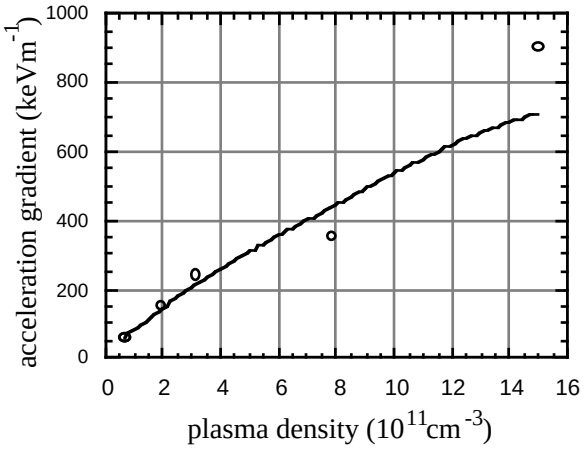

Figure. 5. Dependence of acceleration gradient on plasma density. Solid line shows prediction of a linear theory.

Calculated and experimental value of wakefield are shown in Fig. 6. The experimental value is estimated from beam images on SC1, SC2 and SC3, assumed linear field and thin lens. Figure 7 shows the dependence of beam sizes at the maximum focusing phase on the plasma density. The beam sizes were observed at the exit of the energy analyzer. The solid line shows numerical simulation. The experimental value is smaller than the theoretical. The difference between theoretical value and experimental one is due to the displacement of trajectories of the drive bunch and the test bunch.

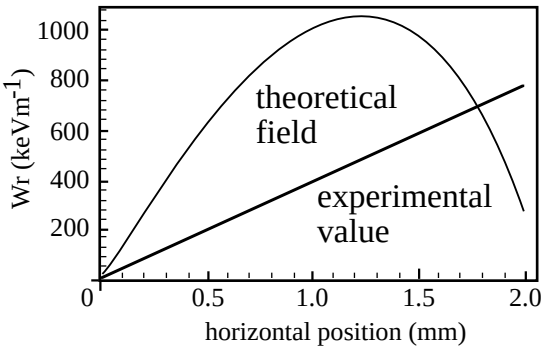

Figure. 6. Transverse wakefield at the maximum focusing phase. Plasma density was $1.5 \times 10^{12} cm^{-3}$.

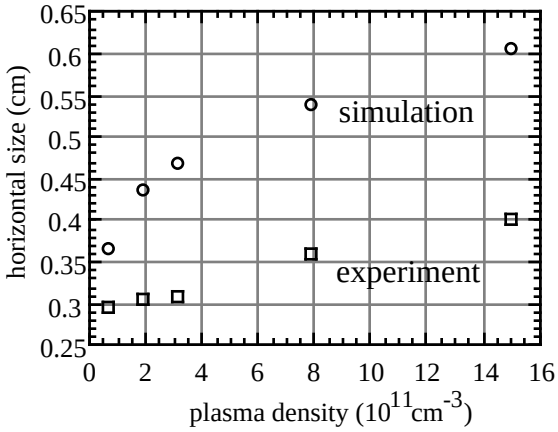

Figure. 7. Dependence of beam sizes at the maximum focusing phase on the plasma density.

References

[1] P. Chen *et al.*, Phys. Rev. Lett. **54**, 693 (1985).

[2] J. Rosenzweig *et al.*, Phys. Rev. Lett. **61**, 98 (1988).

[3] A. Ogata, in AIP Cof. Proc. 279; Advanced Accelerator Concepts, Port Jefferson, New York, 1992, edited by J. Wurtele, (American Institute of Physics, New York, 1993) p.420.

[4] H. Nakanishi *et al.*, Nucl. Instr. Meth. **A328**, 596 (1993).

[5] H. Nakanishi *et al.*, Phys. Rev. Lett. **66**, 1870 (1990).

[6] A. Ogata *et al.*, Phys. Scripta, **T52**, 69 (1994).